
Princeton Plasma Physics Laboratory

PPPL-

PPPL-



Prepared for the U.S. Department of Energy under Contract DE-AC02-09CH11466.

Princeton Plasma Physics Laboratory

Report Disclaimers

Full Legal Disclaimer

This report was prepared as an account of work sponsored by an agency of the United States Government. Neither the United States Government nor any agency thereof, nor any of their employees, nor any of their contractors, subcontractors or their employees, makes any warranty, express or implied, or assumes any legal liability or responsibility for the accuracy, completeness, or any third party's use or the results of such use of any information, apparatus, product, or process disclosed, or represents that its use would not infringe privately owned rights. Reference herein to any specific commercial product, process, or service by trade name, trademark, manufacturer, or otherwise, does not necessarily constitute or imply its endorsement, recommendation, or favoring by the United States Government or any agency thereof or its contractors or subcontractors. The views and opinions of authors expressed herein do not necessarily state or reflect those of the United States Government or any agency thereof.

Trademark Disclaimer

Reference herein to any specific commercial product, process, or service by trade name, trademark, manufacturer, or otherwise, does not necessarily constitute or imply its endorsement, recommendation, or favoring by the United States Government or any agency thereof or its contractors or subcontractors.

PPPL Report Availability

Princeton Plasma Physics Laboratory:

<http://www.pppl.gov/techreports.cfm>

Office of Scientific and Technical Information (OSTI):

<http://www.osti.gov/bridge>

Related Links:

[U.S. Department of Energy](#)

[Office of Scientific and Technical Information](#)

[Fusion Links](#)

Edge plasma boundary layer generated by kink modes in tokamaks

Leonid E. Zakharov

PPPL, Princeton University, Princeton NJ, 08543 USA

(November 4, 2010)

This paper describes the structure of the electric current generated by external wall touching and free boundary kink modes at the plasma edge using the ideally conducting plasma model. Both kinds of modes generate a δ -functional surface current at the plasma edge. Free boundary kink modes also perturb the core plasma current, which in the plasma edge compensates the difference between the δ -functional surface currents of free boundary and wall touching kink modes. In addition, the resolution of an apparent paradox with the pressure balance across the plasma boundary in the presence of the surface currents is provided.

I. INTRODUCTION

Recently the important role of electric currents due to kink modes at the plasma edge of tokamaks was understood. When the plasma column, which initially is in magneto-hydrodynamic (MHD) equilibrium, is deformed it requires special external fields to maintain the equilibrium. Without them, the surface currents would be excited at the plasma edge in order to eliminate the normal component of magnetic field to the plasma boundary [1–3]. Fig.1 illustrates this statement for the case of a straight plasma column with the current I_{pl} in the longitudinal magnetic field B_ϕ , where plasma is deformed by the $m/n = 1/1$ kink mode (m, n are poloidal and toroidal wave numbers).

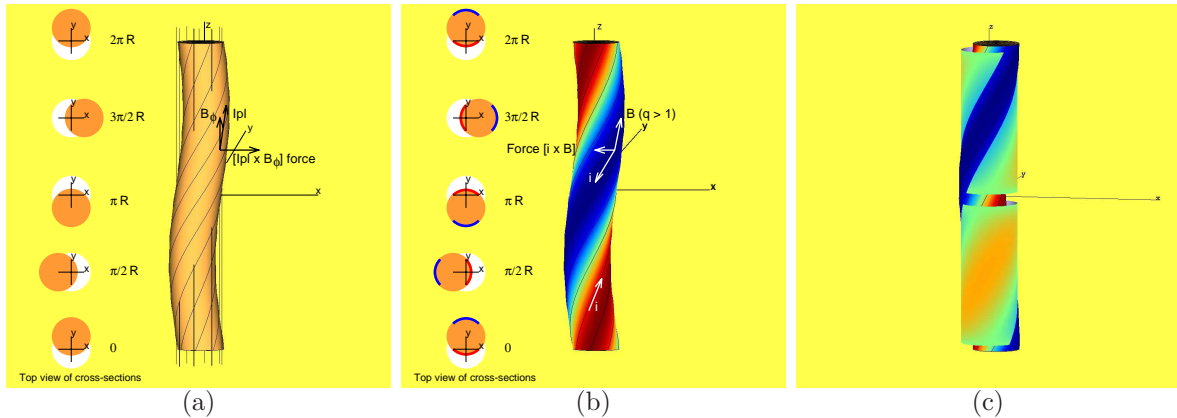


FIG. 1. (a) Toroidal magnetic field lines punch the plasma surface; (b) Surface currents eliminate B_{norm} : █ opposite to I_{pl} , █ in the direction of I_{pl} ; (c) Hiro currents in the wall are always opposite to I_{pl} . The eddy currents remain localized (red spot) inside the wall sectors.

Fig.1(a) shows the existence of the normal field component B_{norm} if there would be no surface currents. This situation is not consistent with the properties of the high temperature plasma, which instead always excites surface (not necessary δ -functional) currents. For the $1/1$ kink mode their direction is shown in Fig.1(b) with blue indicating current in opposite to the plasma current I_{pl} direction and red in the same direction as I_{pl} .

The surface currents are always negative at the plasma side moving toward the wall. As a result, after touching the wall, the surface currents at the plasma boundary will be shared with the wall in the form of negative Hiro currents, as is illustrated in Fig.1(c) regardless the gaps in the wall. This creates a new regime for MHD instabilities, called the wall touching kink mode (WTKM) [3].

In the case of the $m/n = 1/1$ WTKM the negative Hiro currents in the wall explain the asymmetry in the plasma current measurements in JET [4–6]. There is every reason to expect that the same Hiro currents can explain the positive current spike in internal plasma current measurements in conventional disruptions as well.

Because of Hiro currents, the physics of the plasma edge and plasma-wall interactions is of the great importance for plasma dynamics during disruptions. Recently, the first step in this direction was made in Ref. [7]. In particular, it was determined that for the free boundary kink modes (not WTKM) the surface currents remain δ -functional (as in the perturbed equilibrium theory) even taking into account the finite growth rate. They always flow along the field lines.

In this paper, the simplest model of the plasma edge, based on the ideal linear MHD approximation is presented as a reference case for future models. The circular cross-section plasma in the strong longitudinal magnetic field is considered as a simplest case revealing the properties of the plasma edge. In Sect. 2 the basic set of equations is specified. Sect. 3 describes the δ -functional surface currents for both WTKM and free boundary kink modes (FBKM).

Sect. 4 describes the perturbations of the plasma current in both modes and the boundary layer of the FBKM. The analytical expressions for characteristics of the boundary layer are obtained. In particular, they correct one of the estimates of the δ -functional current given earlier [7]. Sect. 5 explains the mechanism, compensating the component of surface current perpendicular to the magnetic field and resolves the apparent inconsistency between direction of surface currents along the field lines and the periodicity constraint. The Appendix contains corrections to some technical mistakes in Ref. [7].

II. LINEARIZED MHD EQUATIONS

The linearized MHD equations are well-known [8–11]. For a stratified model of a tokamak plasma column in a strong magnetic field we for simplicity follow the recent Ref. [7].

We consider the straight cylinder case as a basic approximation for a toroidal plasma and accordingly use $r, \omega, R\phi$ ($0 \leq r \leq a$) as cylindrical coordinates with a, R being minor and major radii of toroidal plasma and perturbations of the form

$$r = \bar{r} + \xi(r)e^{\gamma t} \cos(m\omega - n\phi), \quad (1)$$

where \bar{r} is the cylindrical radius of the unperturbed magnetic surface. The perturbation of the magnetic field $\tilde{\mathbf{B}}$ can be specified as [12]

$$\tilde{\mathbf{B}} = \tilde{B}_r \mathbf{e}_r + \tilde{B}_\omega \mathbf{e}_\omega + \tilde{B}_\phi \mathbf{e}_\phi = \nabla\psi \times \mathbf{e}_\phi + \tilde{B}_\phi \mathbf{e}_\phi, \quad \tilde{B}_r = \frac{1}{r}\psi'_\omega, \quad \tilde{B}_\omega = -\psi'_r. \quad (2)$$

The perturbation of vector potential ψ and plasma displacement ξ are related through

$$\psi = B_\omega^* \xi, \quad B_\omega^* \equiv B_\omega - \frac{nr}{mR} B_\phi = \frac{B_\phi}{R} r \mu^*, \quad (3)$$

where we introduced notations

$$\mu^*(r) \equiv \mu - \frac{m}{n}, \quad \mu(r) \equiv \frac{1}{q(r)} = \frac{RB_\omega}{rB_\phi}, \quad (4)$$

The function $\mu^*(r)$ is the same as Δ in Eq. (32) of Ref. [7].

In terms of normalized growth rate $\tilde{\gamma}$ and variable η

$$\tilde{\gamma}^2 \equiv \frac{\mu_0 \rho \gamma^2 R^2}{m^2 B_\phi^2}, \quad \eta \equiv r\xi, \quad (5)$$

where ρ is the plasma density (assumed to be uniform), and μ_0 is the vacuum magnetic permeability, the linearized equation determining η and ψ has the form [7]

$$\left[r(\tilde{\gamma}^2 + \mu^{*2})\eta' \right]' = \frac{m^2}{r}(\tilde{\gamma}^2 + \mu^{*2})\eta + (\mu^{*2})'\eta, \quad \psi = \frac{B_\phi}{R}\mu^*\eta. \quad (6)$$

In the vacuum outside the plasma

$$\psi^v = \frac{\frac{a^m}{r^m} - \lambda^m \frac{r^m}{a^m}}{1 - \lambda^m} \frac{B_\phi}{R} \mu_a^* \eta_a, \quad \frac{a\psi'^v(a)}{\psi^v} = -m - \frac{2m\lambda^m}{1 - \lambda^m}, \quad \lambda \equiv \frac{a^2}{b^2}, \quad (7)$$

where λ takes into account the presence of the wall with radius b .

The growth rate is determined by the matching condition obtained by integrating Eq. (6) across the plasma boundary

$$(\tilde{\gamma}^2 + \mu^{*2}) \frac{a\eta'}{\eta} \Big|_a = \mu_a^{*2} \frac{a\eta'^v}{\eta} = \mu_a^{*2} \frac{a\psi'^v}{\psi^v} - \mu_a^* a\mu'^v = (2\mu_a - m\mu_a^*)\mu^* - \frac{2m\lambda^m}{1 - \lambda^m} \mu_a^{*2}. \quad (8)$$

The perturbation \tilde{B}_ξ of the poloidal component of magnetic field at the perturbed magnetic surface is determined by

$$\tilde{B}_\xi = \tilde{B}_\omega + B'_\omega(r)\xi = -\psi' + B'_\omega(r)\xi = \frac{B_\phi}{R} \left(\mu - \mu^* \frac{r\eta'}{\eta} \right) \xi. \quad (9)$$

The difference $\tilde{B}_\xi^v - \tilde{B}_\xi^c$ between perturbed magnetic fields at the vacuum and core sides of the plasma surface represents the δ -functional surface current $\bar{i}^{surf} \equiv \mu_0 i^{surf}$ excited by the kink mode

$$\bar{i}^{surf} = \tilde{B}_\xi^v - \tilde{B}_\xi^c = \frac{B_\phi}{R} \left[-\frac{jR}{B_\phi} + \left(\frac{r\psi'}{m\psi} + 1 + \frac{2\lambda^m}{1-\lambda^m} \right) m\mu^* \right] \xi_a, \quad (10)$$

or

$$\bar{i}^{surf} = \frac{B_\phi}{R} \left[-2\mu + \left(\frac{a\eta'}{m\eta} + 1 + \frac{2\lambda^m}{1-\lambda^m} \right) m\mu^* \right] \xi_a. \quad (11)$$

The Ref. [7], Eq. (29) has suggested also an expression in terms of the growth rate when η' is substituted by the eigen-value $\tilde{\gamma}^2$ using the boundary condition Eq. (8)

$$\bar{i}^{surf} = \frac{B_\phi}{R} \frac{\tilde{\gamma}^2}{\tilde{\gamma}^2 + \mu^{*2}} \left[-2\mu + \left(1 + \frac{2\lambda^m}{1-\lambda^m} \right) m\mu^* \right] \xi_a. \quad (12)$$

The important property of surface currents i^{surf} at the plasma boundary is that they do not contain a common resonant factor $m\mu_a^* = m\mu_a - n$ in their amplitude and are finite at the stability boundary $m\mu_a = n$. These currents vanish only at another marginal stability point $nq_a = nq_L < m$, which is determined by the current distribution and geometry of the stabilizing wall. In contrast, the eddy currents i^{eddy} in the wall, which are generated by the perturbation of magnetic field outside the plasma $\tilde{B}_r = \mathbf{B} \cdot \nabla \xi$ (\mathbf{B} is the equilibrium magnetic field), do have the resonant factor $m\mu_a^*$ in their amplitude. Using Eq. (7) the expression for i^{eddy} on a cylindrical wall can be obtained as

$$\bar{i}^{eddy} \equiv \mu_0 i^{eddy} = -\tilde{B}_\omega(b) = -m\mu_a^* \frac{B_\phi}{R} \frac{2}{1-\lambda^m} \frac{a^m}{b^m} \frac{\eta_a}{b}. \quad (13)$$

The eddy currents are always much smaller than the surface current at the plasma as well as the Hiro currents in the WTKM.

III. SURFACE CURRENTS OF THE WALL TOUCHING AND FREE BOUNDARY KINK MODES

In the wall touching kink mode regime the plasma core remains in MHD equilibrium. The force acting on the surface currents, which are converted into Hiro currents in the wall, is applied to the wall. The core equilibrium can be described by Eq. (6) with $\tilde{\gamma}^2 = 0$ or, alternatively, by the perturbed equilibrium equation for vector potential ψ

$$\Delta \Psi^* = 2 \frac{nB_\phi}{mR} - \bar{j}(\Psi^*), \quad \Psi^* = \Psi_0^*(r) + \psi, \quad B_\omega^* = -\Psi_0^{*'}, \quad (r\psi')' = \frac{m^2}{r} \psi + \frac{R\bar{j}'}{B_\phi \mu^*} \psi, \quad \bar{j} \equiv \mu_0 j, \quad (14)$$

where $j(r)$ is the toroidal current density.

The individual kink modes m/n do not represent the WTKM (see, Ref. [3]) in the real situation. At the same time, they serve as the elementary components of WTKM and their properties are important. For conventional free boundary kink modes, FBKM, the surface currents are in equilibrium but the core is not in equilibrium and $\tilde{\gamma}^2$ is determined as an eigen-value by Eqs. (6, 8).

The kink mode $m = 1$ is a special case, specific for cylindrical and toroidal geometry. The solution to both Eq. (6) and Eq. (14) is simply

$$\eta = \frac{r}{a} \eta_a, \quad \psi = \mu^*(r) \frac{r}{a} \frac{B_\phi}{R} \eta_a \quad (15)$$

and the surface current Eq. (10,11) for both WTKM and FBKM is given by

$$\bar{i}_{m=1}^{surf} = -2 \frac{B_\phi}{R} \left[n - \frac{\lambda}{1-\lambda} (\mu_a - n) \right] \xi_a, \quad (16)$$

where $\lambda = a^2/b^2$ takes into account the effect of eddy currents in the wall. At $\mu_a \simeq n$ the eddy currents are not excited and their effect is absent.

For kink modes $m > 1$, a special case with an analytical solution to both Eq. (6) and Eq. (14) is represented by a uniform plasma current distribution $j_\phi = \text{const}$ ($\mu = \text{const}$):

$$\eta = \frac{r^m}{a^m} \eta_a, \quad \psi = \mu^* \frac{B_\phi}{R} \frac{r^m}{a^m} \eta_a, \quad \frac{r\eta'}{m\eta} = \frac{r\psi'}{m\psi} = 1. \quad (17)$$

Then, Eq. (10,11) gives the value of the surface current

$$\bar{i}_{\bar{j}=\text{const}}^{surf} = 2 \frac{B_\phi}{R} \left[(m-1)\mu_a - n + \frac{\lambda^m}{1-\lambda^m} (m\mu_a - n) \right] \xi_a. \quad (18)$$

In calculations of i^{surf} (10,11) for non-uniform plasma current profiles $a\eta'/\eta$ or $a\psi'/\psi$ should be obtained from a numerical solution of Eqs. (6,14). In the examples below the following current distribution $j(r)$ is used

$$\frac{R}{B_\phi} \bar{j} = \frac{4\mu_a}{1+j_1} \left[1 - (1-j_1) \frac{r^2}{a^2} \right], \quad \mu(r) = \frac{4\mu_a}{1+j_1} \left[\frac{1}{2} - (1-j_1) \frac{r^2}{4a^2} \right], \quad (19)$$

where $\mu_a = \mu(a) = 1/q_a$ and $j_1 = j(a)/j(0)$. The case $j_1 = 1$ corresponds to the uniform plasma current distribution. The results are presented in terms of a dimensionless form \hat{i}^{surf} of the surface current and $\hat{\gamma}$, normalized to the poloidal Alfvén transit time, as defined by the relationships

$$\hat{i}^{surf} = \frac{q_a R}{\xi_a B_\phi} \cdot \bar{i}^{surf} = \frac{a}{\xi_a B_\omega} \cdot \bar{i}^{surf}, \quad \hat{\gamma}^2 \equiv \tilde{\gamma}^2 m^2 q_a^2, \quad (20)$$

with \hat{i}^{surf} equal to $\hat{\sigma}$ of Ref. [7].

Fig. 2 shows the growth rate and amplitudes of \hat{i}_{WTKM}^{surf} and \hat{i}_{FBKM}^{surf} for WTKM and free-boundary kink modes, calculated for $m = 2, 3, 4$ and different values of the j_1 parameter, which controls the edge value of the current density. The eddy current effect in the wall is neglected, $\lambda = 0$. The Cbcyl code, based on `lsode()` routine [13], was created for these calculations.

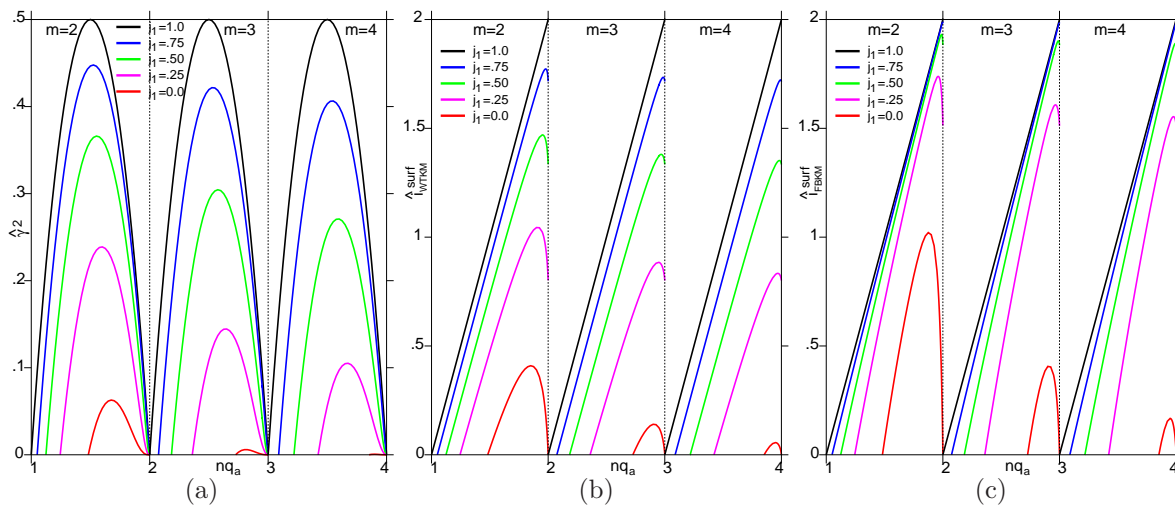


FIG. 2. (a) Growth rate $\hat{\gamma}^2$ of free boundary kink modes; (b) Normalized surface current $-\hat{i}_{WTKM}^{surf}$ (with the opposite sign) for WTKM; (c) Normalized surface currents and $-\hat{i}_{FBKM}^{surf}$ for free boundary kink modes. Stabilizing wall is absent.

For a parabolic current distribution ($j_1 = 0$) the kink mode $m = 4$ is practically marginally stable (Fig. 2). Its maximum growth rate is $\hat{\gamma}^2 \simeq 0.0006$.

The surface currents are equal to zero at the left boundary $nq_a = nq_L$ of the instability zone on the nq_a axis for each separate mode (Fig. 2a), but are finite at the resonant value $nq_a = m$.

Note, that the value of \hat{i}_{FBKM}^{surf} in Fig. 2c at the resonant point $nq_a = m$ is not equal to a “universal” number 2 of Ref. [7], as could be expected based on assumption that $\hat{\gamma}^2$ is dominant over μ^{*2} in Eq. (12). The behavior of edge currents near the right boundary of the instability zone $nq \rightarrow m$ is considered in the next section in detail.

IV. STRUCTURE OF THE EDGE PLASMA CURRENTS

The previous section has presented the δ -functional part of the edge current, referred to as the surface current. Here, the perturbation of the bulk current, excited by the kink modes near the plasma edge is analyzed as well. The most important case corresponds to the marginal situation near the resonant value of the safety factor $nq_a \simeq m$. In a perturbed equilibrium, corresponding to WTKM, the current density preserves the functional dependence $\bar{j}(\Psi^*)$ or $\bar{j}(\bar{r})$, where \bar{r} is a flux coordinate $r = \bar{r} + \xi \cos(m\omega - n\phi)$, and is not perturbed inside the core. In the laboratory coordinates r, ω, ϕ , the perturbation $\tilde{j}(r)$ of the \bar{j} is given by

$$\bar{j}(\bar{r}) = \bar{j}(r) - \bar{j}'(r)\xi(r) \cos(m\omega - n\phi) \quad (21)$$

and is produced exclusively by the shaping of magnetic surfaces by the kink mode.

The perturbation of the plasma current $\tilde{I}_{WTKM}^{edge}(\bar{r}) \cos(m\omega - n\phi)$ between the plasma boundary (including the surface current) and an internal magnetic surface \bar{r} can be calculated as

$$\tilde{I}_{WTKM}^{edge}(\bar{r}) \equiv a\bar{i}_{WTKM}^{surf} + \int_{\bar{r}}^a \bar{j}(\bar{r})\eta' d\bar{r}. \quad (22)$$

Here, the expression of the surface element dS of the plasma cross-section in flux coordinates \bar{r}, ω, ϕ

$$drd\omega = \frac{D(r, \omega)}{D(\bar{r}, \omega)} d\bar{r}d\omega = [1 + \xi' \cos(m\omega - n\phi)] d\bar{r}d\omega, \quad dS = drd\omega = [\bar{r} + \eta' \cos(m\omega - n\phi)] d\bar{r}d\omega \quad (23)$$

was used. The total perturbed current between the same surfaces in the sector $-\pi/(2m) \leq m\omega - n\phi \leq \pi/(2m)$ is equal to $2\tilde{I}^{edge}/m$.

In contrast to WTKM, free boundary kink modes do perturb the current density inside the core. The substitution $\psi = B_\phi \mu^* \eta / R$ instead of η in all terms, not containing $\tilde{\gamma}^2$ in Eq. (6), leads to the equation

$$(r\psi)' - \frac{m^2}{r}\psi = \frac{R\bar{j}'}{B_\phi \mu^*} \psi - \frac{B_\phi}{R} \frac{r(r\tilde{\gamma}^2 \eta')' - \tilde{\gamma}^2 m^2 \eta}{r\mu^*} = \bar{j}'\xi - \delta\bar{j}, \quad (24)$$

where the right hand side represents the perturbation of the current density in laboratory coordinates. The first term corresponds to the perturbed equilibrium and is due to deformation of an equilibrium plasma as in the WTKM case. It does not contribute to the perturbation of the current density in flux coordinates. The second term is the real perturbation of the current density by the FBKM. Using the same Eq. (6) it can be represented as

$$\delta\bar{j} = \frac{B_\phi}{R} \frac{r(\tilde{\gamma}^2 r \eta')' - \tilde{\gamma}^2 m^2 \eta}{r^2 \mu^*} = 2 \frac{B_\phi}{R} \tilde{\gamma}^2 \frac{\mu'(\eta - r\eta')}{r(\tilde{\gamma}^2 + \mu^{*2})}. \quad (25)$$

Accordingly, the current perturbation for FBKM has the form

$$\tilde{I}_{FBKM}^{edge}(\bar{r}) \equiv a\bar{i}_{FBKM}^{surf} + \int_{\bar{r}}^a (\bar{j}\eta' + \bar{r}\delta\bar{j}) d\bar{r}. \quad (26)$$

Fig. 3 shows the profiles of the normalized perturbed edge plasma current $\hat{I}^{edge}(r)$, defined as

$$\hat{I}_{WTKM}^{edge}(r) \equiv \hat{i}_{WTKM}^{surf} = \text{const}, \quad \hat{I}_{FBKM}^{edge}(r) \equiv \hat{i}_{FBKM}^{surf} + \frac{Rq_a}{B_\phi \xi_a} \int_{\bar{r}}^a \bar{r}\delta\bar{j} d\bar{r}, \quad (27)$$

where the current perturbation due to changes in geometry is excluded. The current profile (19) with $j_1 = 1/7$ corresponds to a fixed value of $q_a \bar{j}_a R / B_\phi = 0.5$ parameter, while different values of $nq_a \rightarrow 2$ for the $m = 2$ mode are shown.

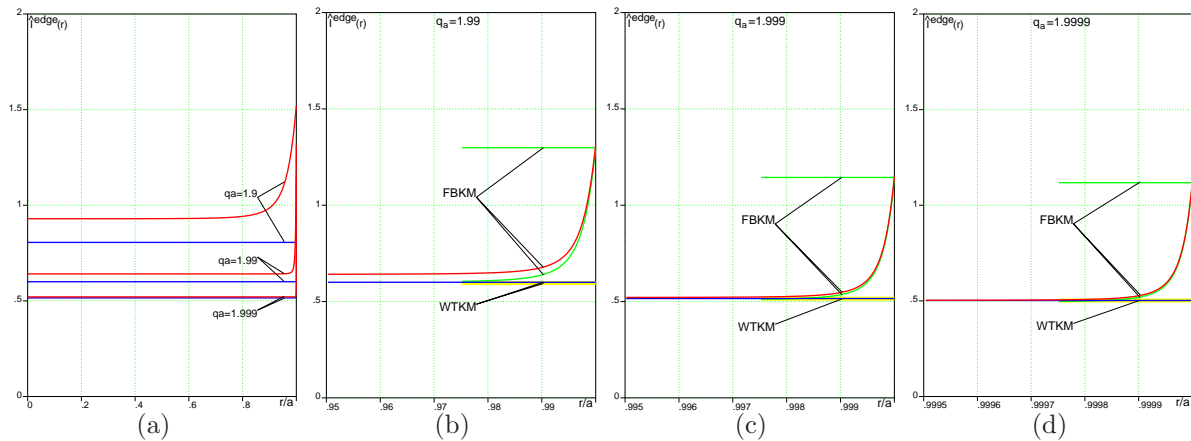


FIG. 3. Normalized edge current $\hat{I}^{edge}(r)$ perturbation for $q_a \bar{J}_a R/B_\phi = 0.5$, $m = 2$ for WTKM (blue curves) and FBKM (red curves). Yellow and green lines are calculated using analytical solutions for \hat{i}_{WTKM}^{surf} and \hat{i}_{FBKM}^{surf} and $\hat{I}_{FBKM}^{edge}(r)$. In calculations, the eddy current effect is neglected, $\lambda = 0$. (a) Full radial profiles $0 \leq r/a \leq 1$ for three cases, $nq_a = 1.9, 1.99, 1.999$; (b) Edge region $0.95 \leq r/a \leq 1$ for $nq_a = 1.99$. (c) $0.995 \leq r/a \leq 1$ for $nq_a = 1.999$. (d) $0.9995 \leq r/a \leq 1$ for $nq_a = 1.9999$.

The boundary layer in FBKM becomes evident at $nq_a \rightarrow 2$ with a limit $\hat{I}_{FBKM}^{edge} \rightarrow \hat{i}_{WTKM}^{surf}$ in the plasma core, which means that the excess of the δ -functional surface current over its perturbed equilibrium value is screened by the perturbation of the bulk current density at the edge region.

Figs. 3b,c,d show the zoomed $\hat{I}^{edge}(r)$ profiles at the plasma edge region together with their asymptotic levels and analytical approximations.

The analytical asymptotic expression, explaining behavior of the surface current \hat{i}^{surf} in Figs. 2,3, can be obtained for both WTKM and free boundary kink modes. For WTKM at $nq \rightarrow m$, and $\mu^* \rightarrow 0$, with logarithmic accuracy the behavior of ψ can be represented by

$$\frac{R}{B_\phi} \psi \simeq 1 + \frac{R \bar{J}_a}{B_\phi \mu'_a} \frac{x}{a} \ln \frac{|x|}{a} + c^{core} x, \quad \frac{R}{B_\phi} a \psi' \simeq \frac{R \bar{J}_a}{B_\phi \mu'_a} \ln \frac{|x|}{a} + a c^{core}, \quad (28)$$

where the variable x is defined as

$$x \equiv r - r_s, \quad \mu_a^* + \mu'_a (r_s - a) = 0, \quad (29)$$

and the constant c^{core} depends on the global solution of Eq. (14) and has no analytical expression. The asymptotic expression (28), known in the theory of the tearing modes (see, e.g., Refs. [14,15]), can be obtained by integrating the asymptotic representation $R \bar{J}' \psi / (B_\phi \mu'_a x)$ of the right hand side in Eq. (14) for $x \ll a$, starting with $\psi = 1$ as a zeroth order approximation (see Appendix B). The constant c^{core} is ignored in this paper. This provides only a logarithmic accuracy of asymptotic expressions.

Substitution of Eq. (28) into Eq. (10) gives the following approximation for \hat{i}_{WTKM}^{surf} for $nq \rightarrow m$

$$\hat{i}_{WTKM}^{surf} \simeq -\frac{R \bar{J}_a}{B_\phi} q_a + \left(\frac{R \bar{J}'_a}{B_\phi \mu'_a} \ln \frac{\mu_a^*}{|a \mu'_a|} + \frac{2\lambda^m}{1 - \lambda^m} \right) (m - nq_a), \quad (30)$$

which is plotted as a yellow horizontal line in Figs. 3b,c,d. For $m - nq < 0.01$, it is identical to the numerical solution for \hat{i}_{WTKM}^{surf} and the yellow line in Figs. 3b,c,d is made broader in order to make it not obscured by the numerical (blue) solution. At $nq_a = m$ this expression reduces to

$$\hat{i}_{WTKM}^{surf}|_{nq_a=m} = -q_a \frac{R \bar{J}_a}{B_\phi} = -2 \frac{\bar{J}_a}{\langle \bar{j} \rangle}, \quad (31)$$

where $\langle \bar{j} \rangle$ is the cross-section averaged value of the unperturbed plasma current density.

For free boundary kink modes, the asymptotic value of \hat{i}_{FBKM}^{surf} and $\hat{I}_{FBKM}^{edge}(r)$ -profile can be obtained based on asymptotic behavior of solution $\eta(r)$ to Eq. (6)

$$\eta \simeq \frac{r}{r_s \tilde{\gamma}} \arctan \frac{\tilde{\gamma}}{\mu^*(r)} + \frac{R \bar{J}'_a}{2 B_\phi \mu_a'^2} \ln \frac{\tilde{\gamma}^2 + \mu^{*2}(r)}{a^2 \mu_a'^2} + \frac{c^{core}}{\mu_a'}. \quad (32)$$

This expression can be obtained by assuming $\tilde{\gamma} \propto \mu^* \ll 1$ and integrating the asymptotic representation $2\mu'^2 x \eta$ of the right hand side in Eq. (6) as is shown in Appendix B.

At $\mu^* \gg \tilde{\gamma}$ this solution reproduces the asymptotic behavior expected from WTKM solution (28) for ψ

$$\eta = \frac{R\psi}{B_\phi \mu^*} \rightarrow \frac{1}{\mu' x} + \frac{Rj'}{B_\phi a \mu'^2} \ln \frac{|x|}{a} + \mathcal{O}(1). \quad (33)$$

The substitution of this solution (neglecting the logarithmic term) into the boundary condition Eq. (8) leads to the equation determining the asymptotic value of growth rate $\tilde{\gamma}$ at $\mu^* \rightarrow 0$

$$\dot{\gamma} \equiv \frac{\tilde{\gamma}}{\mu_a^*}, \quad \frac{\arctan \dot{\gamma}}{\dot{\gamma}} = \frac{2\mu_a - j_a}{2\mu_a} = \frac{aq_a^c}{2q_a}, \quad (34)$$

with its numerical solution presented in Fig. 4.

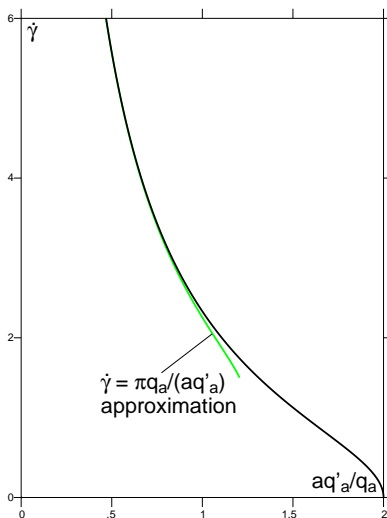


FIG. 4. Eigen-value for growth rate $\dot{\gamma} \equiv \tilde{\gamma}/\mu_a^*$ of FBKM at $nq \rightarrow m$ as a function of the edge shear parameter aq'_a/q_a .

Unlike the case of a uniform current distribution, where $\tilde{\gamma}^2 \propto \mu_a^*$, in all other cases $\tilde{\gamma} \propto \mu_a^*$. Because of this, in Eq. (12) for the surface current of FBKM its asymptotic value at $\mu_a^* \rightarrow 0$ should be obtained using the solution of Eq. (34), rather than simply neglecting μ_a^{*2} compared to $\tilde{\gamma}^2$. Instead of -2 as estimated in Ref. [7], the asymptotic value of \hat{i}_{FBKM}^{surf} is given by

$$\hat{i}_{FBKM}^{surf} \rightarrow \frac{\dot{\gamma}^2}{\dot{\gamma}^2 + 1} \left(-2 + m - nq_a + \frac{2\lambda(m - nq_a)}{1 - \lambda^m} \right) \simeq \frac{-2\dot{\gamma}^2}{\dot{\gamma}^2 + 1}. \quad (35)$$

The analytical approximation of the FBKM edge current, presented by the be green curves in Figs. 3b,c,d, is based on expression (27)

$$\hat{I}_{FBKM}^{edge}(r) \simeq \hat{i} + \frac{r_s q_a}{a \eta_a} \left(\frac{\mu'_a r_s \mu^*}{\tilde{\gamma}^2 + \mu^{*2}} - \frac{\mu'_a r_s}{\tilde{\gamma}} \arctan \frac{\tilde{\gamma}}{\mu^*} + \frac{\tilde{\gamma}^2}{\tilde{\gamma}^2 + \mu^{*2}} \right)_r^a, \quad r_s = a - \frac{\mu_a^*}{\mu'_a} \quad (36)$$

with the use of analytical representation (32) for $\eta(r)$. As in the case of WTKM, the analytical representation is practically identical to the numerical solution for $m - nq_a < 0.01$.

The unstable free boundary kink modes creates a boundary layer with the characteristic width

$$\Delta_{FBKM}^{edge} = \dot{\gamma} x_s \simeq \dot{\gamma} \frac{m - nq_a}{nq_a^c}, \quad x_s \equiv r_s - a. \quad (37)$$

Returning to the edge current of the FBKM, Fig. 5 shows the tendencies in the edge current profile depending on the edge current density in an equilibrium configuration.

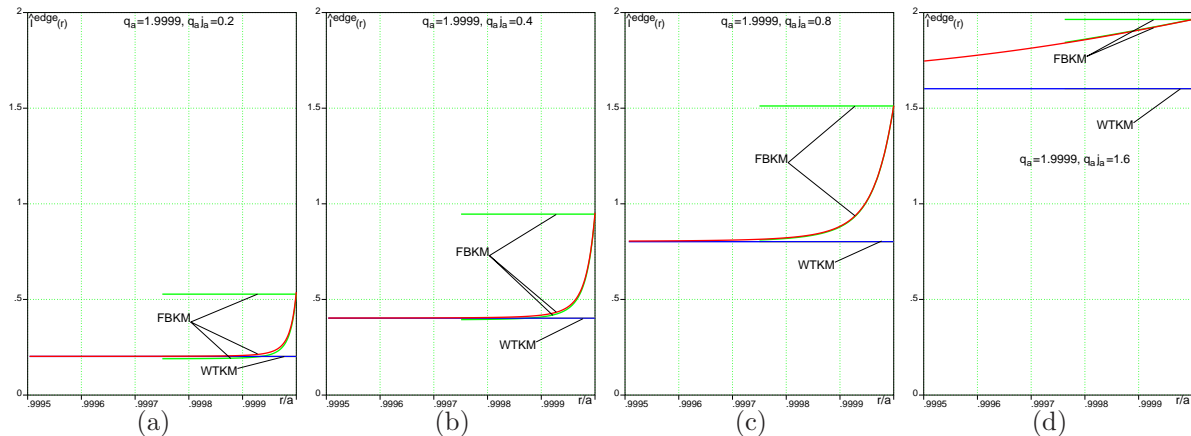


FIG. 5. Normalized edge current $\hat{I}_{FBKM}^{edge}(r)$ in $0.999 \leq r/a \leq 1$ for $q_a = 1.9999$, $m = 2$ and different $q_a \bar{j}_a$ for WTKM and FBKM. Color lines have the same meaning as in Fig. 3. (a) $q_a \bar{j}_a = 0.2$; (b) $q_a \bar{j}_a = 0.4$; (c) $q_a \bar{j}_a = 0.8$; (d) $q_a \bar{j}_a = 1.6$.

For finite μ'_a the perturbation of the edge current in FBKM due to a finite growth rate is localized at the plasma edge.

V. SURFACE CURRENT SUPPLY FROM THE PLASMA CORE

The surface currents, calculated from condition $B_{norm} = 0$, serve as a virtual “super-conducting” casing for the plasma core in WTKM, providing its equilibrium. At the same time the force $\vec{i}^{surf} \times \mathbf{B}$ is acting on the surface currents themselves. In the case of WTKM, this force is applied to the wall. In the case of FBKM, the force would be applied to the plasma surface, unless the surface current are flowing along the field lines, as is noticed in Ref. [7].

The surface currents described previously, and in particular from solution of Eq. (6) are directed along the ignorable coordinate $\phi + nr\omega/(Rm)$, $(\mathbf{e}_\phi + nr/(Rm)\mathbf{e}_\omega) \cdot \nabla = 0$. They have no sources

$$\vec{i}^{surf} = (\nabla I \times \mathbf{n}), \quad \nabla_{\omega, \phi} \cdot \vec{i}^{surf} = 0, \quad (38)$$

where $I = I(\omega, \phi)$ is the stream function of \vec{i}^{surf} and \mathbf{n} is the unit normal vector to the plasma surface. For a single FBKM

$$\vec{i}^{surf} = i^{surf} \left(\mathbf{e}_\phi + \frac{nq}{mR} \mathbf{e}_\omega \right). \quad (39)$$

Some apparent paradox is that because of periodicity condition for $I(\omega, \phi)$ these surface currents always intersect the magnetic field lines (unless $nq = m$), thus, experiencing a force, which should be absent.

Let us remind that Eq. (6) is obtained by applying the operator $\nabla \times$ to the linearized equations of motion

$$\rho \frac{\partial \mathbf{V}}{\partial t} + \nabla p = (\mathbf{j} \times \mathbf{B}), \quad (40)$$

and, thus, contains not a complete information. In addition, there is a compression of the toroidal magnetic field, which generates the poloidal current in the core

$$\mu_0 \mathbf{j}^{pol} = (\nabla \tilde{B} \times \mathbf{e}_\phi), \quad \mu_0 j_r^{pol} = \frac{1}{r} \frac{\partial \tilde{B}}{\partial \omega}, \quad \mu_0 j_\omega^{pol} = -\frac{\partial \tilde{B}}{\partial r}. \quad (41)$$

This current is small in comparison with the toroidal component of the perturbed current, but is essential for the force balance because it is interacting with the strong longitudinal field. The explicit expression for j_r^{pol} can be obtained from the projection of equation of motion on ignorable direction (\mathbf{e}_ϕ in our approximation)

$$j_r^{pol} B_\omega = j_\omega \tilde{B}_r, \quad B_\omega \tilde{B} = j_\omega \psi. \quad (42)$$

The radial component of the equation of motion

$$\rho \gamma^2 \xi + p'_r = ((\mathbf{j} \times \mathbf{B}) \cdot \mathbf{e}_r), \quad (43)$$

after integration across the plasma surface gives the force balance in terms of the surface currents

$$-p = ((\vec{i} \times \mathbf{B}) \cdot \mathbf{n}) = ((\vec{i}^{surf} \times \mathbf{B}) \cdot \mathbf{n}) + ((\vec{i}_\omega \times \mathbf{B}_\phi) \cdot \mathbf{n}). \quad (44)$$

In contrast to \vec{i}^{surf} , the current \vec{i}_ω have a source in the normal component of the bulk radial current $j_r \mathbf{e}_r$ flowing to the plasma boundary from the core

$$\mu_0 i_\omega \equiv \mu_0 \int_{a-\geq}^a j_\omega dr = -\mu_0 \int^\omega d\omega \int_{a-\geq}^a (r j_r)'_r dr = \tilde{B}, \quad (45)$$

which is consistent with the contribution of i_ω into the force balance across the plasma surface [10]

$$((\vec{i}_\omega \times \mathbf{B}_\phi) \cdot \mathbf{n}) = \frac{B\tilde{B}}{\mu_0} = \frac{B^2|c - B^2|v}{2\mu_0}. \quad (46)$$

VI. SUMMARY

Calculation of the structure of the edge plasma region perturbed by free boundary kink modes revealed a boundary current layer, consisting from the δ -functional surface currents and the edge localized plasma bulk current perturbations. For non-uniform current profiles the perturbation of the core current density near the edge compensates partially the δ -functional surface current, thus making the total edge current perturbation in FBKM equal to the surface current of WTKM.

The analytical expressions for the marginal cases $nq_a \simeq m$ are obtained for both growth rates, surface currents of WTKM and FBKM and for the edge current profiles. In particular, it is shown that for non-uniform plasma current distribution the growth rate of FBKM is proportional to $m - nq_a$, rather than $\sqrt{m - nq_a}$ as in the case of uniform current. It is also explained that in the case of free boundary kink mode the force acting on the surface currents, excited by the plasma deformation, is compensated by the force acting on the poloidal component of the surface current, which has a source in the plasma core in the form of the perturbation of the toroidal magnetic field.

Acknowledgment. This work is supported by US DoE contract No. DE-AC02-09-CH11466.

APPENDIX A: CORRECTIONS TO CALCULATIONS OF REF. [7]

Fig. 6 represents recalculations (using Cbcy1) of data presented in 3 figures of Ref. [7] for the current distribution specified by the safety factor $q(r)$ -profile as

$$q(r) = q_0 + q_1 \frac{r^2}{a^2}. \quad (A1)$$

The following notations from Ref. [7], used in figures, are defined as

$$bc(\tilde{\gamma}) \equiv -(\tilde{\gamma}^2 + \mu_a^{*2}) \frac{a\eta'}{\eta} + (2\mu_a - m\mu_a^*)\mu_a^*, \quad \frac{a\hat{\sigma}}{\xi_a} \equiv \hat{i}_{FBKM}^{surf}. \quad (A2)$$

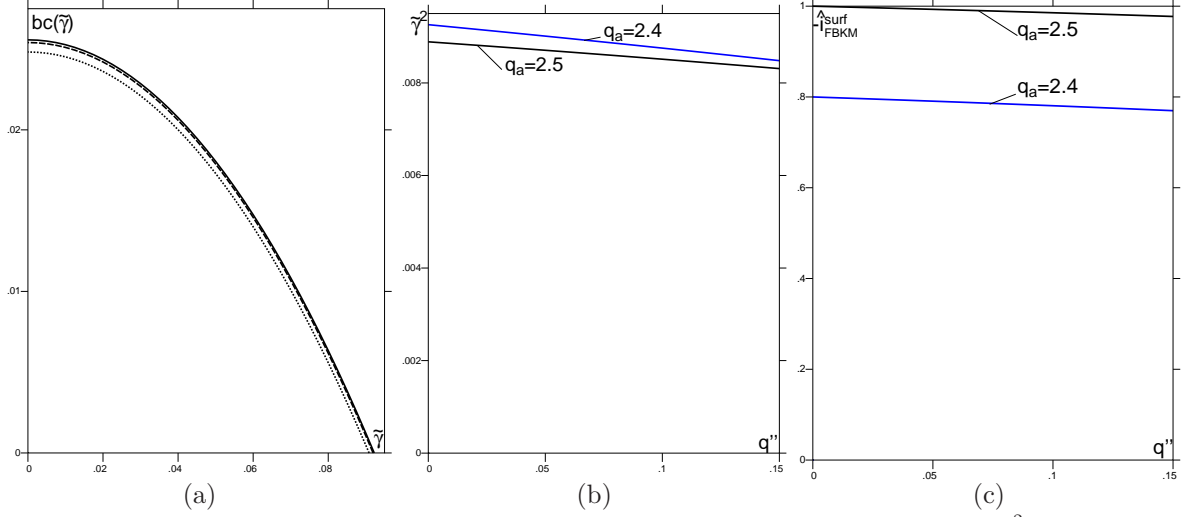


FIG. 6. (a) Boundary condition $bc(\tilde{\gamma})$ vs $\tilde{\gamma}$ (recalculated Fig. 1 of Ref. [7]); (b) Growth rate $\tilde{\gamma}^2$ of FBKM $m = 3$ as function of q'' in Eq. (A1) for $q_a = 2.5$ and $q_a = 2.4$ (recalculated Fig. 2 of Ref. [7]); (c) Surface current $-a\hat{\sigma}/\xi_a = -\hat{i}_{FBKM}^{surf}$ for $m = 3$ as function of q'' for $q_a = 2.5$ and $q_a = 2.4$ (recalculated Fig. 3 of Ref. [7]).

APPENDIX B: DERIVATION OF ASYMPTOTIC SOLUTIONS FOR WTKM AND FBKM

At $nq_a \rightarrow m$, the distance x from the resonant surface $r = r_s$ can be used as a small parameter in Eq. (14) for WTKM, which can be approximated by

$$(a\psi')' \simeq \frac{D}{x}\psi, \quad x = r - r_s, \quad D \equiv \frac{R\vec{j}_a}{B_\phi\mu'_a}. \quad (\text{B1})$$

With $\psi_0 = 1$ as the main approximation [14,15], the next approximation ψ_1 can be obtained by integration of the right hand side

$$a\psi'_1 \simeq D \ln \frac{|x|}{a} + ac^{core} + D, \quad \psi_1 = D \frac{x}{a} \ln \frac{|x|}{a} + c^{core}x, \quad (\text{B2})$$

where c^{core} is a constant of integration.

In the case of the FBKM, the expansion parameter at $\mu^* \rightarrow 0$ can be $\tilde{\gamma} \propto \mu_a^*$ and the first term in the right hand side of Eq. (eq:gh) can be ignored. Then, introducing a new independent variable t as a dimensionless coordinate, the leading term and the next order correction in the solution η are determined by

$$\eta = \eta_0 + \eta_1, \quad \mu^{*2} = \mu_s'^2 x^2 (1 + sx), \quad s \equiv \frac{\mu_a''}{\mu_a'}, \quad x \equiv \frac{\tilde{\gamma}}{\mu_s'} t, \quad \mu_s' \equiv \mu_a' + s\mu_a^*, \quad (\text{B3})$$

$$\mu_a'^2 \frac{d}{dt} \left[\left(1 + t^2 + \tilde{\gamma} \frac{st^3}{\mu'} \right) \left(1 + \tilde{\gamma} \frac{t}{a\mu_a'} \right) r_s \frac{d\eta_0}{dt} \right] = 0, \quad \mu_a'^2 \frac{d}{dt} \left[(1 + t^2) r_s \frac{d\eta_1}{dt} \right] = 2\tilde{\gamma}\mu_a' t \eta_0. \quad (\text{B4})$$

The first integration of equation for η_0 gives

$$\frac{d\eta_0}{dt} = -\frac{1}{1+t^2} + \frac{\tilde{\gamma}st^3}{\mu_a'(1+t^2)^2} + \frac{\tilde{\gamma}t}{a\mu_a'(1+t^2)}. \quad (\text{B5})$$

The next integration gives

$$\eta_0 = \arctan \frac{1}{t} + \frac{\tilde{\gamma}s}{2\mu_a'(1+t^2)} + \frac{\tilde{\gamma}(1+sr_s)}{2a\mu'} \ln(1+t^2) + \hat{\gamma}C^{core}, \quad (\text{B6})$$

where only the first term corresponds to the leading order. Using it in the equation for η_1

$$\frac{d}{dt} \left[(1+t^2) \frac{d\eta_1}{dt} \right] = 2\tilde{\gamma} \frac{t}{a\mu_a'} \arctan \frac{1}{t}, \quad (\text{B7})$$

the correction η_1 can be calculated as

$$(1+t^2)\eta'_1 = \tilde{\gamma} \frac{1+t^2}{a\mu'_a} \arctan \frac{1}{t} + \tilde{\gamma} \frac{t}{a\mu'_a}, \quad \eta_1 = \frac{\tilde{\gamma}}{a\mu'_a} t \arctan \frac{1}{t} + \frac{\tilde{\gamma}}{a\mu'_a} \ln(1+t^2). \quad (\text{B8})$$

Finally, after returning to the x coordinate, all together can be combined in a compact representation

$$\eta = \frac{r}{r_s} \arctan \frac{\tilde{\gamma}}{\mu^*} + \frac{\tilde{\gamma}D}{2\mu'a} \ln \frac{\tilde{\gamma}^2 + \mu^{*2}}{\mu'^2 a^2} + C^{core}. \quad (\text{B9})$$

Multiplied by a common factor $1/\tilde{\gamma}$ this expression was used in section IV.

- [1] L. E. Zakharov, Sov. J. Plasma Phys. **7**, 8 (1981).
- [2] L. E. Zakharov and V. D. Shafranov. *Reviews of Plasma Physics* Edited by Acad. M.A. Leontovich, (Consultant Bureau, New York, 1986), Vol.11, p.153.
- [3] L. E. Zakharov. Phys. of Plasmas, **15**, 062507 (2008).
- [4] P. Noll, P. Andrew, M. Buzio, R. Litunovski, T. Raimondi, V. Riccardo, and M. Verrecchia, in *Proceedings of the 19th Symposium on Fusion Technology, Lisbon*, edited by C. Varandas and F. Serra (Elsevier, Amsterdam, 1996), Vol. 1, p. 751.
- [5] V. Riccardo, P. Noll, and S. P. Walker, Nucl. Fusion **40**, 1805 (2000).
- [6] V. Riccardo and S. P. Walker, Plasma Phys. Controlled Fusion **42**, 29 (2000).
- [7] A. J. Webster. Phys. of Plasmas, **17**, TBD (2010).
- [8] M. A. Leontovich, V.D. Shafranov. In *“Plasma Physics and the Problem of Controlled Thermonuclear Reactions”*, edited by Acad. M. A. Leontovich. (Pergamon Press, New York-Oxford-London-Paris 1961) Vol. 1, p. 255.
- [9] I. B. Bernstein, E. A. Frieman, M. D. Kruskal, and R. M. Kulsrud, Proc. Roy. Soc. (London) **A244**, 17 (1958).
- [10] B.B. Kadomtsev. In *“Reviews of Plasma Physics, 1966”*, Edited by Acad. M.A. Leontovich, (Consultants Bureau, New York) Vol. 2 153.
- [11] J.P. Freidberg, *“Ideal Magnetohydrodynamics”*, (New York, Plenum Press, 1987).
- [12] B.B. Kadomtsev, O.P. Pogutse. Zh. Eksp. Teor. Fiz., **65** 575 (1973)
- [13] A. Hindmarsh, in *Scientific Computing*, edited by R. Stepleman (North-Holland, Amsterdam, 1983).
- [14] H.P. Furth, J. Killeen, and M.N. Rosenbluth. Phys. Fluids, **6**, 459 (1963).
- [15] H.P. Furth, P.H. Rutherford, and H. Selberg. Phys. Fluids, **16**, 1054 (1973).

The Princeton Plasma Physics Laboratory is operated
by Princeton University under contract
with the U.S. Department of Energy.

Information Services
Princeton Plasma Physics Laboratory
P.O. Box 451
Princeton, NJ 08543

Phone: 609-243-2245
Fax: 609-243-2751
e-mail: pppl_info@pppl.gov
Internet Address: <http://www.pppl.gov>